Electronic Supplementary Information

Reversible Photoactivation in Coordination Polymer-derived CdS/Co-N Species Composites for Enhanced Photocatalytic Hydrogen Evolution

Yuxiao Guo†, Yawei Yang†, Xingtian Yin*, Jie Liu, and Wenxiu Que*

Electronic Materials Research Laboratory, Key Laboratory of the Ministry of Education & International Center for Dielectric Research, and Shaanxi Engineering Research Center of Advanced Energy Materials and Devices, School of Electronic Science and Engineering, Xi'an Jiaotong University, Xi'an 710049, P. R. China

† These authors contributed equally to this work.

* Corresponding authors: xt_yin@mail.xjtu.edu.cn (X. Yin) wxque@mail.xjtu.edu.cn (W. Que)

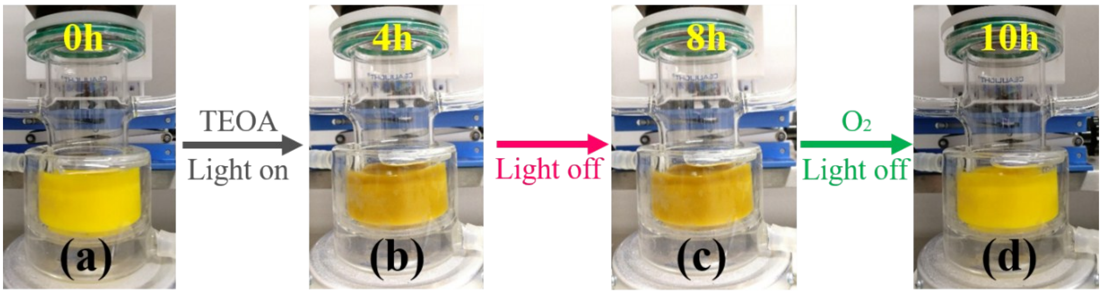

Fig. S1 Photos of the Cd_3TMT_2-400 sample during HER process: (a) initial state, (b) after 4 h irradiation, (c) after another 4 h without irradiation, and (d) after another 2 h O_2 introduction.

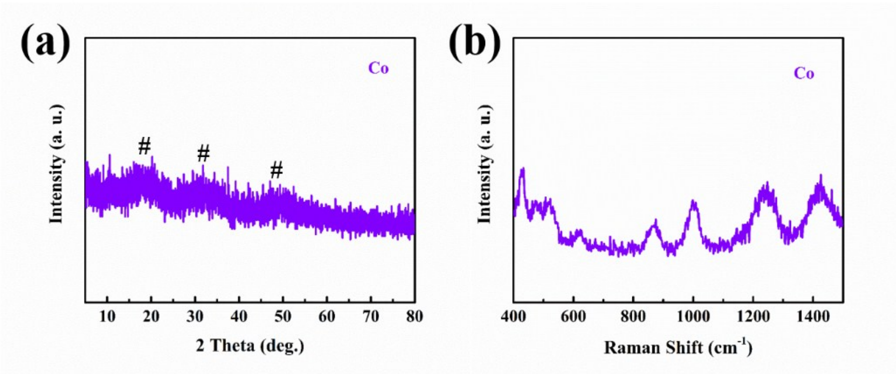

Fig. S2 (a) XRD pattern and (b) Raman spectra of the $Co_3(TMT)_2$ coordination polymer.

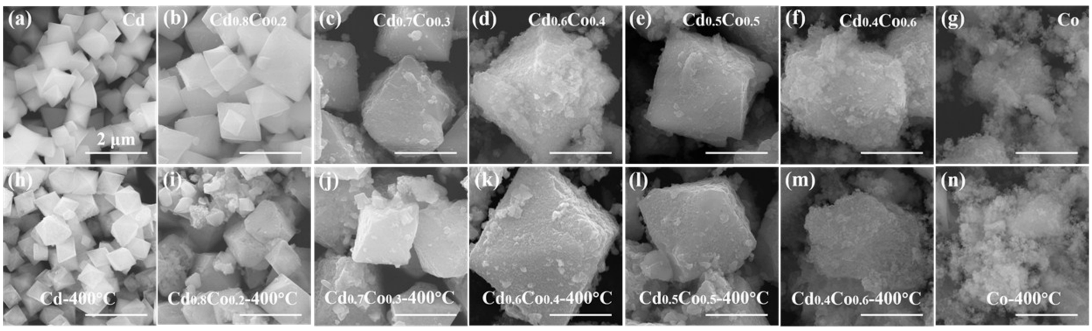

Fig. S3 SEM images of the $(Cd_{1-x}Co_x)_3TMT_2$ coordination polymers and the corresponding 400 °C pyrolysis products.

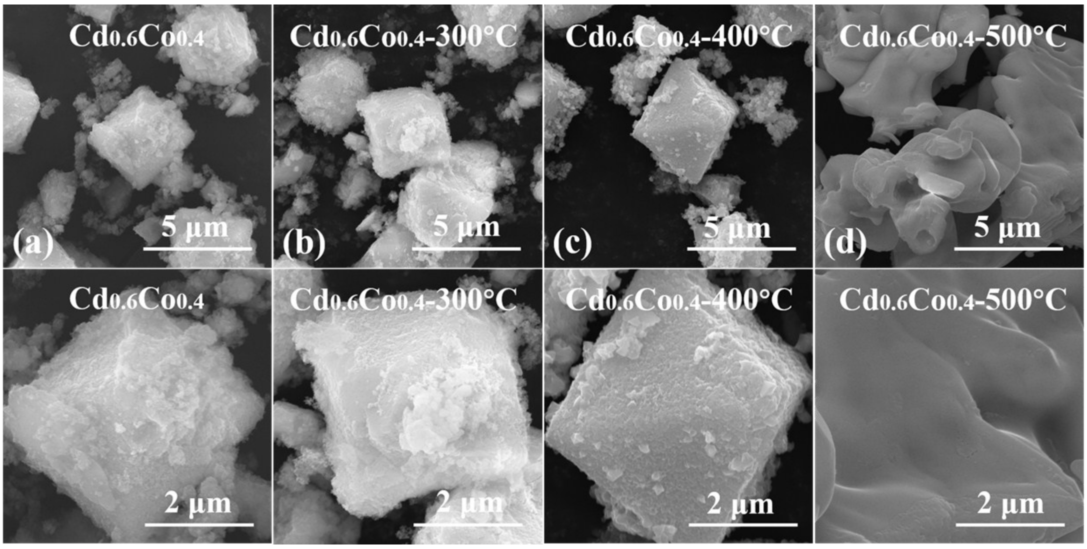

Fig. S4 SEM images of the $(Cd_{0.6}Co_{0.4})_3TMT_2$ coordination polymers and corresponding pyrolysis products.

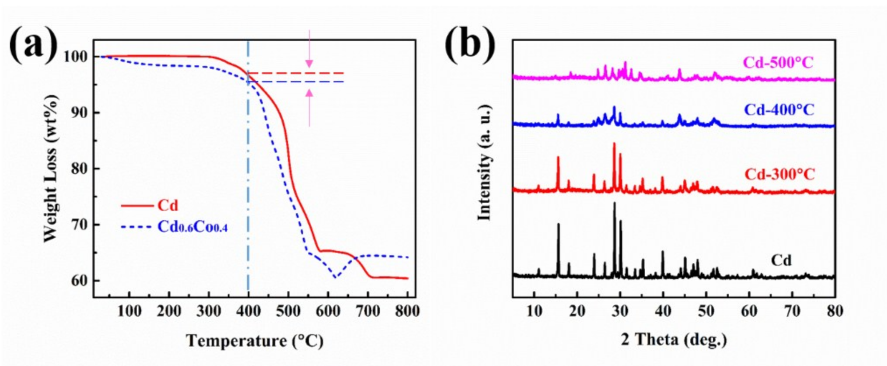

Fig. S5 (a) TGA curves of the Cd_3TMT_2 and $(Cd_{0.6}Co_{0.4})_3TMT_2$ coordination polymers in air, and (b) XRD patterns of the Cd_3TMT_2 pyrolysis products.

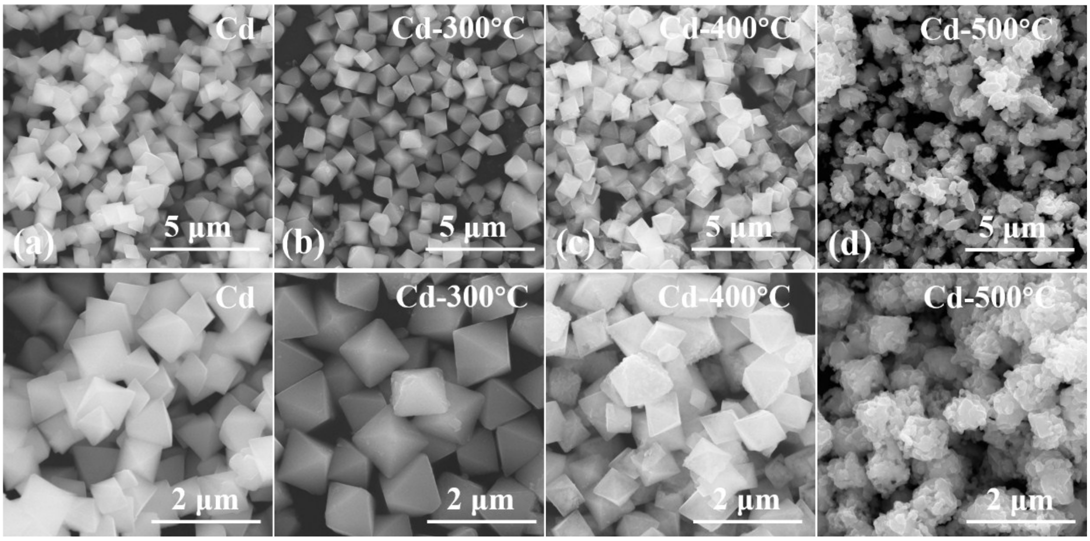

Fig. S6 SEM images of the Cd_3TMT_2 coordination polymers and corresponding pyrolysis products.

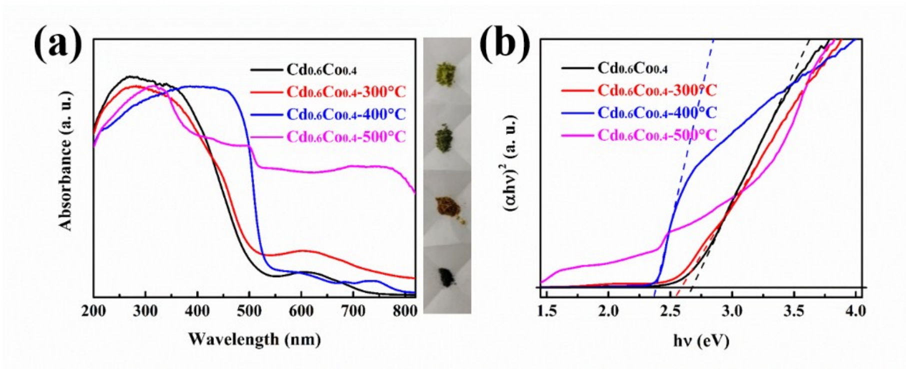

Fig. S7 (a) UV-vis diffuse reflectance absorption spectra and (b) estimated bandgaps of the $(Cd_{0.6}Co_{0.4})_3TMT_2$ pyrolysis products.

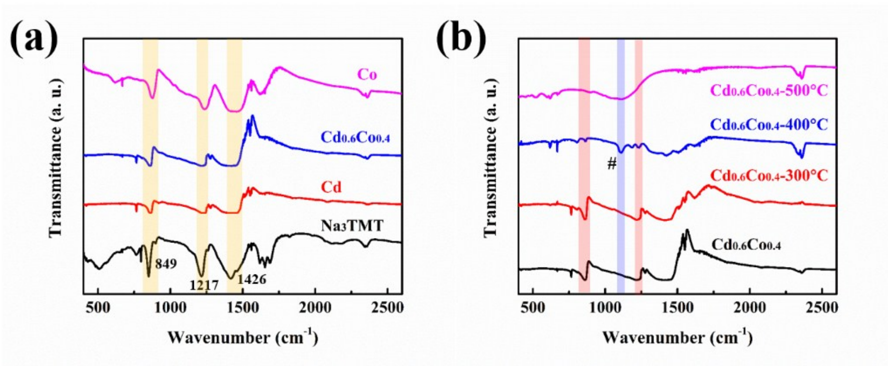

Fig. S8 FTIR spectra of (a) the $(Cd_{1-x}Co_x)_3TMT_2$ coordination polymers and (b) the $(Cd_{0.6}Co_{0.4})_3TMT_2$ pyrolysis products.

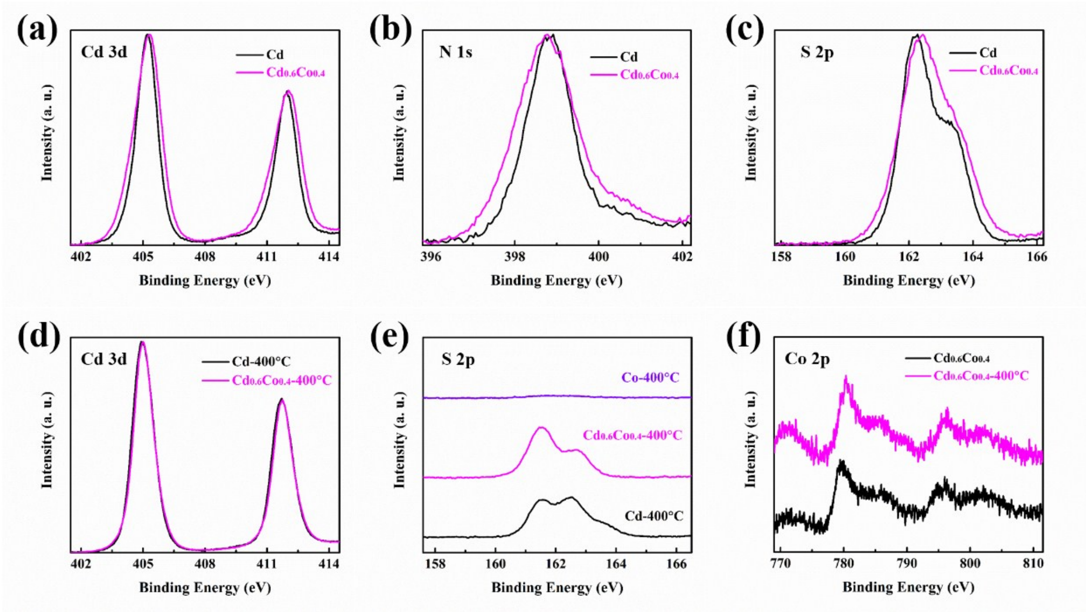

Fig. S9 XPS spectra of the Cd_3TMT_2, $(Cd_{0.6}Co_{0.4})_3TMT_2$, and Co_3TMT_2 coordination polymers and their corresponding 400 °C pyrolysis products: (a) and (d) Cd 3d, (b) N 1s, (c) and (e) S 2p, and (f) Co 2p regions.

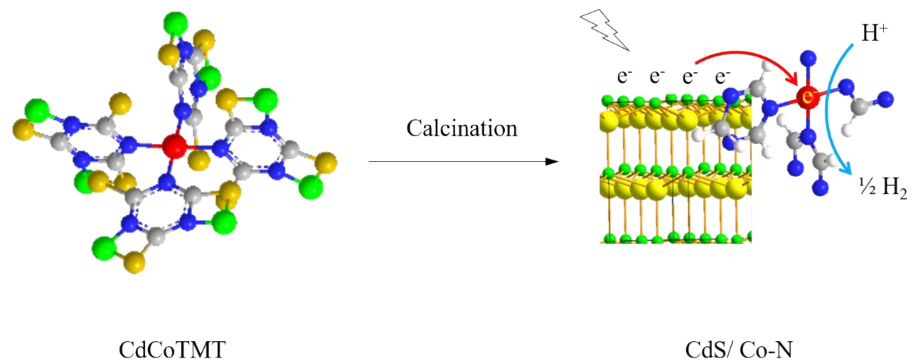

Fig. S10 Structural diagrams for the $(Cd_{0.6}Co_{0.4})_3TMT_2$ coordination polymer and the corresponding 400 ºC pyrolysis product.

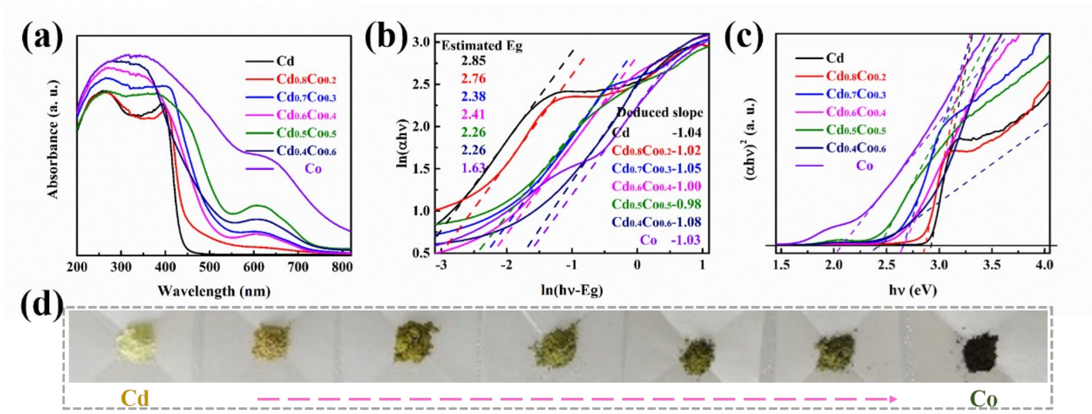

Fig. S11 (a) UV-vis diffuse reflectance absorption spectra, (b) corresponding ln(αhv) *vs.* ln(hv-*E*g) plots, (c) estimated bandgaps and (d) photos of the $(Cd_{1-x}Co_x)_3TMT_2$ coordination polymers.

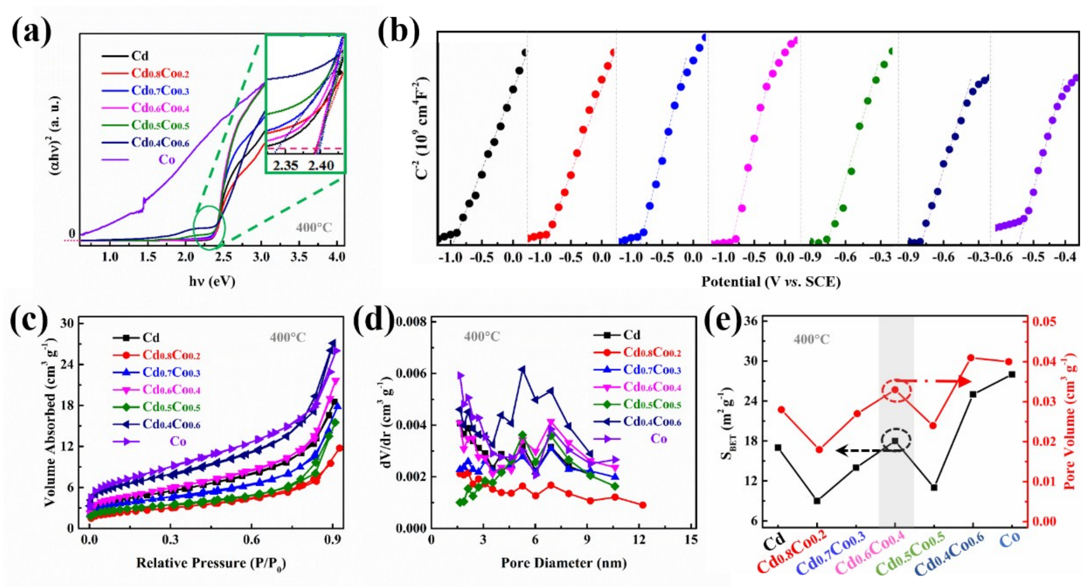

Fig. S12 (a) Estimated bandgaps, (b) Mott-Schottky plots, and (c-e) Nitrogen adsorption-desorption isotherm and Barrett-Joyner-Halenda (BJH) pore size distribution of the $(Cd_{1-x}Co_x)_3TMT_2$-400 samples.

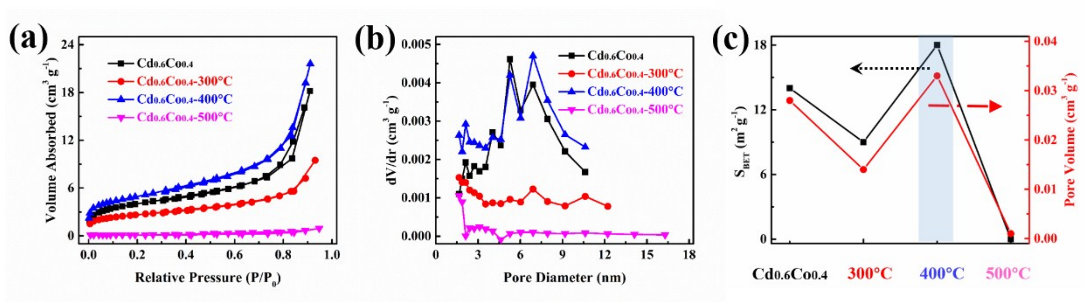

Fig. S13 (a-c) Nitrogen adsorption-desorption isotherm and Barrett-Joyner-Halenda (BJH) pore size distribution of the $(Cd_{0.6}Co_{0.4})_3TMT_2$ pyrolysis products.

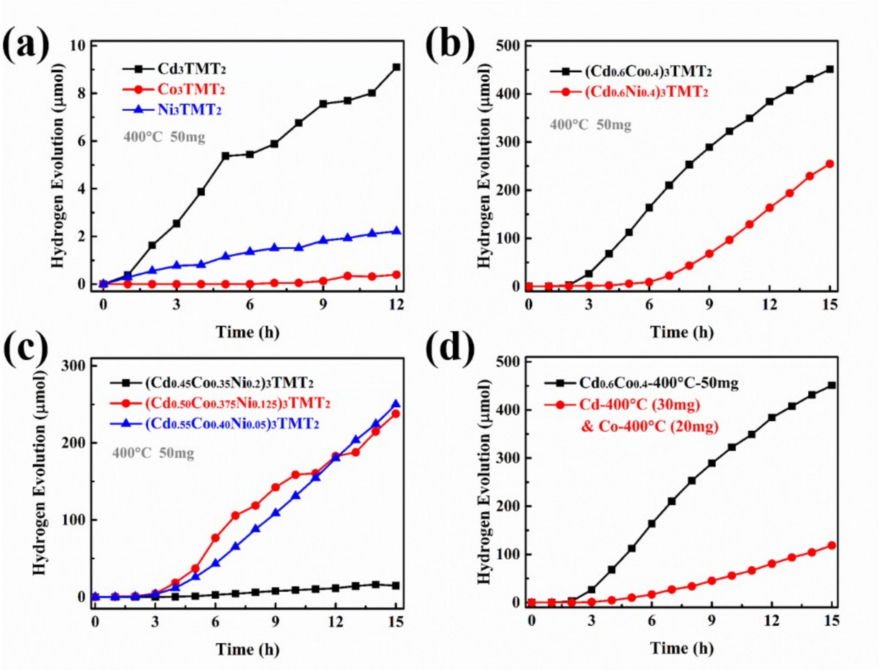

Fig. S14 Photocatalytic hydrogen evolution amounts of the 400 °C pyrolysis products from: (a) the Cd_3TMT_2, Co_3TMT_2 and Ni_3TMT_2, (b) the $(Cd_{0.6}Co_{0.4})_3TMT_2$ and $(Cd_{0.6}Ni_{0.4})_3TMT_2$, and (c) the $(Cd_{0.45}Co_{0.35}Ni_{0.2})_3TMT_2$, $(Cd_{0.50}Co_{0.375}Ni_{0.125})_3TMT_2$ and $(Cd_{0.55}Co_{0.40}Ni_{0.05})_3TMT_2$; (d) Hydrogen evolution of the $(Cd_{0.6}Ni_{0.4})_3TMT_2$-400 and mechanically mixed Co_3TMT_2-400/Cd_3TMT_2-400 = 4/6 sample.

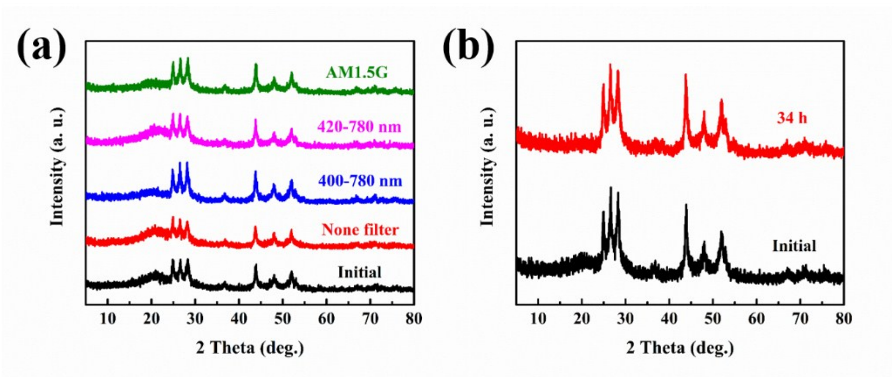

Fig. S15 XRD patterns of the $(Cd_{0.6}Co_{0.4})_3TMT_2$-400 samples before and after photocatalytic hydrogen evolution reaction: (a) under various light spectra: none, 400-780 nm, 420-780 nm and AM1.5G filters, and (b) after 34 h reaction.

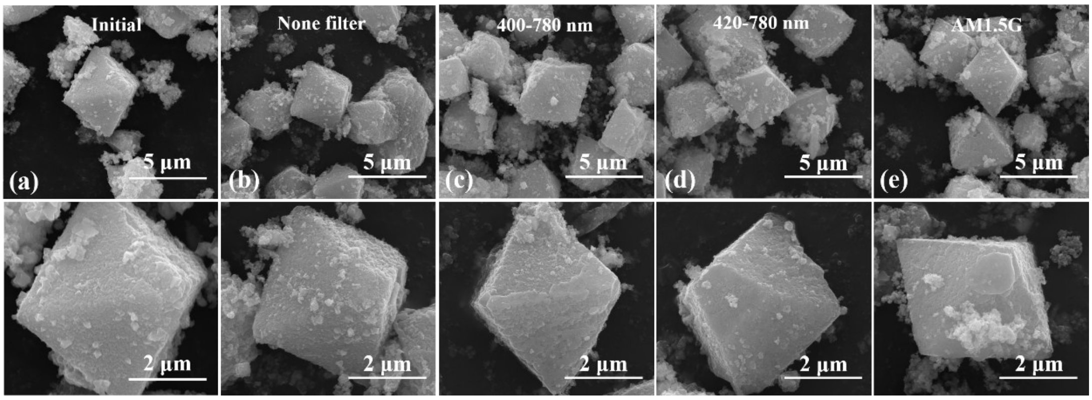

Fig. S16 SEM images of the $(Cd_{0.6}Co_{0.4})_3TMT_2$-400 samples before and after photocatalytic hydrogen evolution reaction under various light spectra: none, 400-780 nm, 420-780 nm and AM1.5G filters.

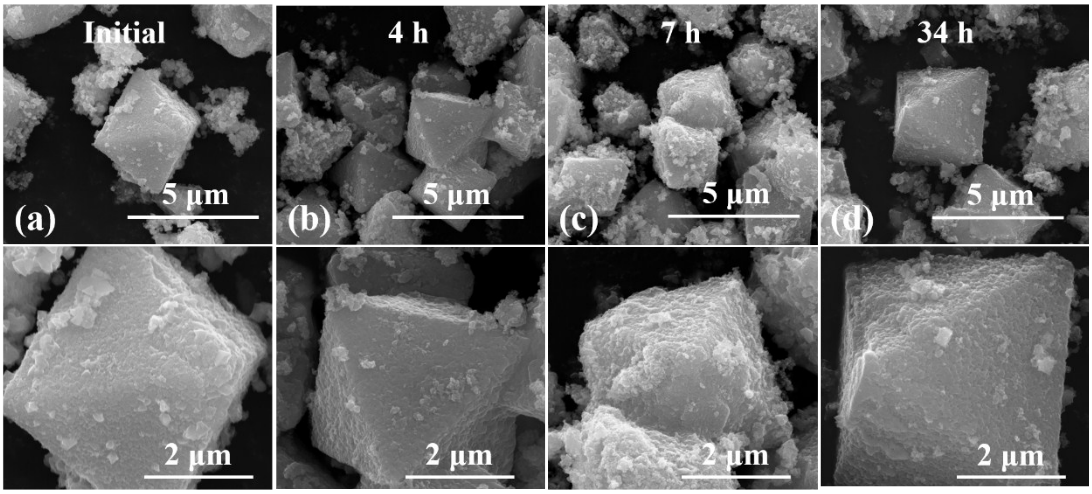

Fig. S17 SEM images of the $(Cd_{0.6}Co_{0.4})_3TMT_2$-400 samples before and after photocatalytic hydrogen evolution reaction for 4 h, 7 h and 34 h.

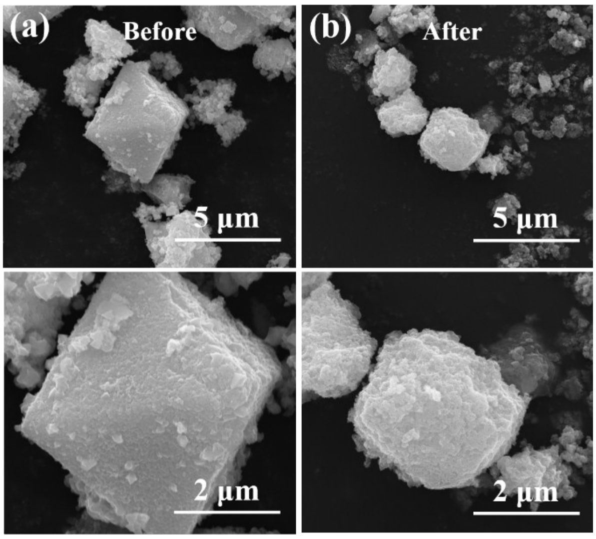

Fig. S18 SEM images of the $(Cd_{0.6}Co_{0.4})_3TMT_2$-400 samples (a) before and (b) after 180 h running.

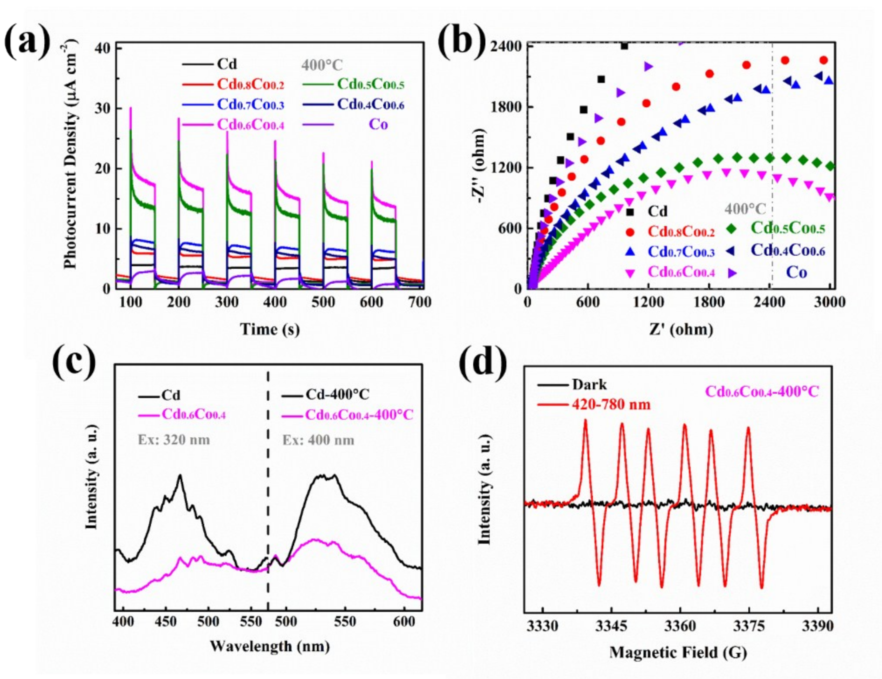

Fig. S19 (a) Photocurrent responses and (b) electrochemical Nyquist plots of the $(Cd_{1-x}Co_x)_3TMT_2$-400 samples; (c) steady-state PL spectra of the Cd_3TMT_2 and $(Cd_{0.6}Co_{0.4})_3TMT_2$ and their corresponding 400 °C pyrolysis products; (d) DMPO-trapped ESR spectra for the $(Cd_{0.6}Co_{0.4})_3TMT_2$-400 sample.

Table S1 The exact Co^{2+}/Cd^{2+} ratios of the $(Cd_{1-x}Co_x)_3TMT_2$-400 samples calculated from XPS results.

Sample	Cd	$Cd_{0.8}Co_{0.2}$	$Cd_{0.7}Co_{0.3}$	$Cd_{0.6}Co_{0.4}$	$Cd_{0.5}Co_{0.5}$	$Cd_{0.4}Co_{0.6}$	Co
Co/Cd atomic ratio	0/100	5/95	6/94	8/92	10/90	15/85	100/0

Table S2 The specific surface area and pore volume of the $(Cd_{0.6}Co_{0.4})_3TMT_2$ pyrolysis products.

Sample	$Cd_{0.6}Co_{0.4}$	$Cd_{0.6}Co_{0.4}$-300	$Cd_{0.6}Co_{0.4}$-400	$Cd_{0.6}Co_{0.4}$-500
S_{BET} (m^2 g^{-1})	14	9	18	almost 0
Pore volume (cm^3 g^{-1})	0.028	0.014	0.033	0.001

Table S3 The specific surface area and pore volume of the $(Cd_{1-x}Co_x)_3TMT_2$-400 pyrolysis products.

Sample	Cd	$Cd_{0.8}Co_{0.2}$	$Cd_{0.7}Co_{0.3}$	$Cd_{0.6}Co_{0.4}$	$Cd_{0.5}Co_{0.5}$	$Cd_{0.4}Co_{0.6}$	Co
S_{BET} (m^2 g^{-1})	17	9	14	18	11	25	28
Pore volume (cm^3 g^{-1})	0.028	0.018	0.027	0.033	0.024	0.041	0.040

Kinetics fitting in Cd_3TMT_2-400, Cd_3TMT_2-400+MV^{2+}, Cd_3TMT_2-400+PTZ and $(Cd_{0.6}Co_{0.4})_3TMT_2$-400 samples.

The XB and PA kinetics can be fitted to a triple-exponential decay:

$$XB(t) \text{ or } PA(t) = A_1*e^{-t/\tau 1} + A_2*e^{-t/\tau 2} + A_3*e^{-t/\tau 3} \quad \text{(S1)}$$

where A_i and τ_i are the relative amplitude and time constant for the i-th component. The fitting parameters are listed in Table S4.

The averaged charge transfer and recombination time constants (τ_{ave}) are calculated using the following expression:

$$\tau_{ave} = (\tau_1*A_1 + \tau_2*A_2 + \tau_3*A_3) /(A_1+A_2+A_3) \quad \text{(S2)}$$

Table S4 Fitting Parameters for the Cd_3TMT_2-400, Cd_3TMT_2-400+MV^{2+}, Cd_3TMT_2-400+PTZ and $(Cd_{0.6}Co_{0.4})_3TMT_2$-400 samples.

Sample	Signal	τ_1 (ps)/ A_1	τ_2 (ps)/ A_2	τ_3 (ps)/ A_3	τ_{ave} (ps)	$\tau_{1/2}$ (ps)
Cd_3TMT_2-400	XB	12.4/ -0.15	132.8/ -0.24	1137.6/ -0.28	526	737
	PA	5.8/ 0.18	76.4/ 0.26	615.6/ 0.26	259	201
Cd_3TMT_2-400+MV^{2+}	XB	9.0/ -0.18	84.0/ -0.33	699.3/ -0.36	323	135
	PA	7.8/ 0.23	52.0/ 0.20	497.2/ 0.25	201	259
Cd_3TMT_2-400+PTZ	XB	29.7/ -0.18	629.2/ -0.45	629.2/ 0.06	440	954
	PA	4.1/ 2.09	4.1/ -1.83	163.9/ 0.31	91	74
$(Cd_{0.6}Co_{0.4})_3TMT_2$-400	XB	6.5/ -0.20	68.2/ -0.21	607.1/ -0.32	288	370
	PA	1.3/ 0.38	12.3/ 0.28	324.4/ 0.23	88	15